

LIF Spectra of *n*-Propoxy and *i*-Propoxy Radicals and Kinetics of their Reactions with O₂ and NO₂

Ch. Mund, Ch. Fockenberg*), and R. Zellner

Institut für Physikalische Chemie, Universität GH Essen, D-45117 Essen, Germany

Key Words: Atmospheric Chemistry / Chemical Kinetics / Radicals

Fluorescence excitation spectra of CH₃CH₂CH₂O (*n*-propoxy) and (CH₃)₂CHO (*i*-propoxy) radicals were obtained using a combined laser photolysis/laser-induced fluorescence (LIF) technique and the kinetics of reactions of these radicals with (1) O₂ as a function of temperature and with (2) NO₂ as a function of pressure have been determined.

Propoxy radicals were produced by excimer laser photolysis of the appropriate propyl nitrites at λ=351 nm. The spectra of the ($\bar{A} \leftarrow \bar{X}$) transitions show progressions of the CO-stretching vibration in the electronically excited states with spacings of the bands of (560±10) cm⁻¹ for *i*-propoxy and (580±10) cm⁻¹ for *n*-propoxy. Fluorescence spectra taken after excitation in the (4,0) band at λ=340.1 nm (*i*-propoxy) and in the (1,0) band at λ=342.4 nm (*n*-propoxy) show progressions of the CO-stretching vibration in the electronic ground state of (900±60) cm⁻¹ for *i*-propoxy and (1000±50) cm⁻¹ for *n*-propoxy.

The Arrhenius expressions for the reactions of *n*-propoxy and *i*-propoxy with O₂ have been determined to be $k_1(n) = (1.4 \pm 0.6) \times 10^{-14} \exp(-0.9 \pm 0.5 \text{ kJ mol}^{-1}/RT) \text{ cm}^3 \text{ s}^{-1}$ and $k_1(i) = (1.0 \pm 0.3) \times 10^{-14} \exp(-1.8 \pm 0.4 \text{ kJ mol}^{-1}/RT) \text{ cm}^3 \text{ s}^{-1}$ in the range 218–313 K. The rate coefficients for the reactions of NO₂ with *n*-propoxy and *i*-propoxy at *T*=296 K were found to be independent of total pressure with $k_2(n) = (3.6 \pm 0.4) \times 10^{-11} \text{ cm}^3 \text{ s}^{-1}$ (6.7–53 mbar) and $k_2(i) = (3.3 \pm 0.3) \times 10^{-11} \text{ cm}^3 \text{ s}^{-1}$ (6.7–106 mbar).

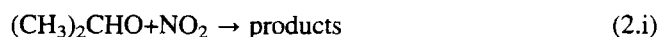
1. Introduction

Alkoxy radicals (RO) are important intermediates in the tropospheric degradation of hydrocarbons. Their subsequent reactions in the troposphere are reaction with O₂, isomerization, decomposition, as well as reaction with NO or NO₂. Whereas oxy radicals from small hydrocarbons mainly react with O₂ and tropospheric trace gases such as NO and NO₂, isomerization and decomposition become more important with increasing number of carbon atoms (>C₄).

Since methane is the most abundant tropospheric trace gas, most of the experiments dealing with alkoxy chemistry have been carried out with methoxy radicals (see e.g. [1–3]). Comparatively few studies have been devoted to the reactions of larger alkoxy radicals. Only one study has been published, in which absolute measurements of the reactions between *i*-propoxy radicals and O₂



and between *i*-propoxy radicals and NO₂,



were performed, using a technique similar to the one applied in the present work [4]. The reaction between *n*-propoxy radicals and O₂,



was studied with relative methods [3, 5] and the reaction of *n*-propoxy radicals and NO₂



was only the topic of thermochemical estimates [6].

In the present work, investigations of both isomers of the propoxy radicals were performed. With the knowledge of the fluorescence properties of these radicals, the application of the LIF technique for kinetic investigations was possible. With this experimental arrangement, rate constants for these reactions could be obtained by measuring time-resolved concentration profiles.

2. Experimental

i-Propoxy and *n*-propoxy radicals were generated by photolysis of the appropriate propyl nitrites using the radiation from an excimer laser (Lambda, EMG 101 MSC) at λ=351 nm (XeF). Following with a certain delay, the propoxy radicals were excited by an excimer-pumped dye laser (Lambda EMG 102 MSC, 308 nm, XeCl and Lambda FL2002). The relative concentration of the radicals was probed by monitoring the fluorescence.

A schematic diagram of the experimental apparatus is shown in Fig. 1. The reaction cell consists of six stainless steel tubes (60 mm diameter) welded to the faces of a drilled stainless steel cube (75 mm length). The photolysis and excitation laser beams counterpropagate collinearly through the two longer arms (300 mm), fixed to opposite faces of the cube. These arms are surrounded by a cooling jacket, allowing the temperature to be regulated in the range 183–313 K using a cryostat with silicone oil as a cooling liquid.

*) Present address: Brookhaven National Laboratory, Chemistry Department, Upton, NY, 11973-5000, USA

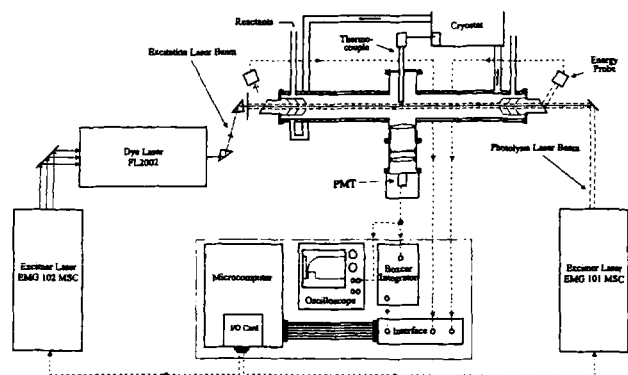


Fig. 1
Schematic representation of laser photolysis/LIF experimental set-up

The fluorescence signal was collected at right angle to the laser beams by a system of lenses, passed through a cut-off filter (Schott, WG-360 nm) and was detected by a PMT (EMI, 9789QB). The signal was integrated by a boxcar averager (Stanford Research, SR252), digitized by an A/D-converter (Stanford Research, SR245) and processed by a personal computer. Approximately 8% of the laser-beam intensity was reflected at the windows, fixed in brewster angle to the reaction cell, and detected by two pyroelectric energy probes (Radiant Dyes, PEM 8). These signals were also transferred to the PC and used for normalizing the fluorescence intensity.

The reactants (NO₂, C₃H₇ONO) used were diluted with He ($x=0.005$ – 0.015) and stored in 20 L glass vessels. The concentrations of the reactants were controlled using flow meters (Tylan, F160) and mixed prior to entering the reaction cell. The overall flow velocity was in the range of 5–15 cm/s at pressures of 6–110 mbar.

The lasers were triggered with 5–8 Hz by the microcomputer (Meilhaus Me14-I/O-card). The delay time between triggering the photolysis and excitation laser was set – dependent on the experiment – within a range of 20–8000 μ s.

Fluorescence excitation spectra were obtained by varying the wavelength of the excitation laser and detecting the integrated fluorescence intensity. The delay between photolysis and excitation was set to 100 μ s, and the signals were averaged over 10 measurements corresponding to 30 points per nm. The spectral regions of 330–350 nm and 345–365 nm were covered using PTP and DMQ, respectively, as laser dyes.

In order to obtain spectra of dispersed fluorescence after excitation at a constant wavelength the experimental set-up was slightly modified. The fluorescence light was collected at right angle by a quartz lens, focused into a monochromator (McPherson 218, 0.3 m focal length, 1200 lines/mm) and detected by a PMT (EMI, 9789 QB). The delay between photolysis and excitation was set constantly to 30 μ s. The signals were averaged over 25 measurements with 3 points per nm generally obtained in the range of 360–560 nm.

Investigations of the fluorescence lifetimes and quenching behaviour of excited propoxy radicals were performed by direct recording of the time-resolved fluorescence signal using a digital storage oscilloscope (LeCroy, LC9414). For acquiring a fluorescence-time profile the fluorescence signal was averaged over 200 measurements in the oscilloscope and finally processed by the microcomputer.

Kinetic measurements were performed with a repetition rate of 5 Hz. The temporal behaviour of the propoxy radicals was registered by recording the LIF intensity as a function of the delay time between photolysis and excitation-laser pulse in the range 20–8000 μ s. Usually an LIF time profile was described by 10–14 single points. In order to enhance the signal-to-noise ratio the whole measurement was repeated 20–150 times, depending on the quality of the signal. The experiments were performed under pseudo-first order conditions with O₂ and NO₂ in at least 20 fold excess.

Propyl nitrites were prepared from a mixture of 35 ml of the appropriate propanol and 40 ml H₂O saturated with NaNO₂. The mixture was dropwise added to 40 ml of 30% H₂SO₄ within 1 h under vivid stirring at 0°C in an Ar atmosphere. After the reaction has finished the pale yellow nitrite phase was purged by an argon stream into a cold trap held at -77°C (*i*-propanol/dry ice). The nitrites were condensed once more into a cold trap and stored at -196°C . The boiling points were found to be 40°C (*i*-propyl nitrite) and 48.5°C (*n*-propyl nitrite).

3. Results and Discussion

3.1 Spectral Properties of *i*- and *n*-Propoxy Radicals

Fig. 2 shows the fluorescence excitation spectrum ($\bar{A} \leftarrow \bar{X}$) of *i*-C₃H₇O radicals (solid curve), which is in excellent agreement to the one observed by Balla et al. [4]. This spectrum could not be observed directly, but had to be corrected for the interference from the fluorescence excitation spectrum of *i*-C₃H₇ONO (see below). The predominant progression ($560 \pm 10 \text{ cm}^{-1}$) of the bands can be assigned to the CO-stretching vibration with the band at 27168 cm^{-1} corresponding to the (0,0) band origin (Table 1). This is in good agreement with the value of 27167 cm^{-1} obtained from the rotational analysis of the laser excitation spectrum of *i*-C₃H₇O by Foster et al. [7]. A series of weaker bands (dotted assignment in Fig. 2) with a spacing of (560 ± 20) cm^{-1} seems to originate from a combined excitation of the CO-stretching vibration and one quantum of another unknown vibration of $\bar{\nu} = (290 \pm 10) \text{ cm}^{-1}$.

A major problem in deriving the fluorescence excitation spectrum of *i*-propoxy was its separation from the excitation spectrum of its photochemical precursor, *i*-propyl nitrite (dotted curve in Fig. 2). Whilst the excitation spectrum of *i*-propyl nitrite is simply obtained from LIF measurements of the parent gas mixture in the absence of photolysing laser radiation, observation of the LIF spectrum of *i*-propoxy required laser photolysis and simulta-

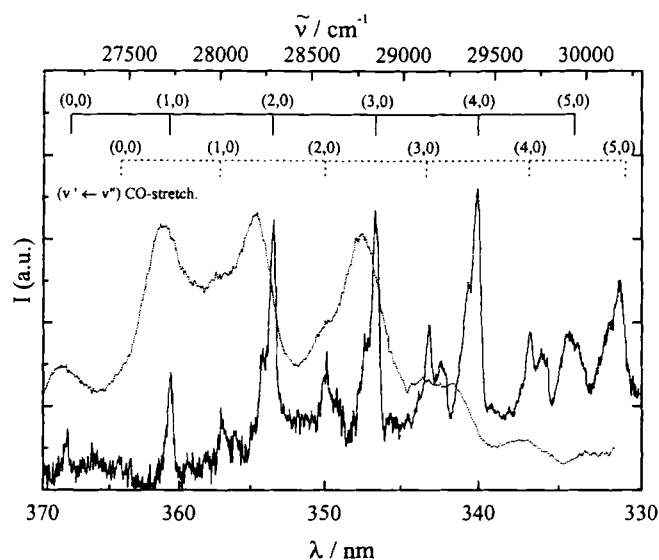


Fig. 2
Fluorescence excitation spectrum ($\bar{A} \leftarrow \bar{X}$) of $i\text{-C}_3\text{H}_7\text{O}$ (solid curve) as derived from the observed spectrum following the photolysis of $i\text{-C}_3\text{H}_7\text{ONO}$ at $\lambda = 351$ nm after background subtraction of the fluorescence excitation spectrum of $i\text{-C}_3\text{H}_7\text{ONO}$ (dotted curve). Intensities have the same scale. $[i\text{-C}_3\text{H}_7\text{ONO}]_0 = 4.0 \times 10^{14} \text{ cm}^{-3}$, $[i\text{-C}_3\text{H}_7\text{O}]_0 = 5 \times 10^{11} \text{ cm}^{-3}$, $T = 295 \text{ K}$, $p = 13.3 \text{ mbar}$

neous background subtraction of the spectrum of the precursor. Since the overlap of the fluorescence excitation spectra of *i*-propyl nitrite itself and *i*-C₃H₇O is minimal in the (4,0) transition, *i*-C₃H₇O was detected in further studies after excitation at 340.1 nm.

Fig. 3 shows the dispersed fluorescence spectrum ($\bar{A} \rightarrow \bar{X}$) after excitation of *i*-C₃H₇O radicals at 340.1 nm. Progressions containing the CO stretching vibration were assigned according to Bai et al. [8]. The determined value of 27111 cm^{-1} for the (0,0) transition agrees well with that obtained from the fluorescence excitation spectrum. The CO stretching frequency was determined to be $(900 \pm 60) \text{ cm}^{-1}$ which indicates, in comparison with the value found in the fluorescence excitation spectra, that the CO bond length is increased in the upper electronic state.

The *n*-C₃H₇O radical fluorescence excitation spectrum ($\bar{A} \leftarrow \bar{X}$) is shown in Fig. 4 (solid curve). Considerably fewer bands can be found compared with *i*-C₃H₇O radicals. The band at 28635 cm^{-1} was assigned to the (0,0) transition of the CO-stretching vibration. The bands showed a spacing of $(580 \pm 10) \text{ cm}^{-1}$ for the CO-stretching vibration in the \bar{A} -state (Table 2). Again a second series of bands may be assigned to the combined excitation of the CO-stretching vibration and another vibration with $\bar{\nu} = (250 \pm 10) \text{ cm}^{-1}$.

Table 1

Band assignment in the fluorescence excitation spectrum ($\bar{A} \leftarrow \bar{X}$) of *i*-C₃H₇O. All transitions are assigned to C-O stretching vibrations. ($v''_{\text{CO}} = 0$; $v''_{\text{unknown vib.}} = 0$)

	$v'_{\text{CO}} =$	0	1	2	3	4	5	6
$\bar{\nu}/\text{cm}^{-1}$	$v'_{\text{unkn.}} = 0$	27168	27730	28294	28845	29398	29941	
$\bar{\nu}/\text{cm}^{-1}$	$v'_{\text{unkn.}} = 1$	27447	28006	28583	29142	29690	30191	

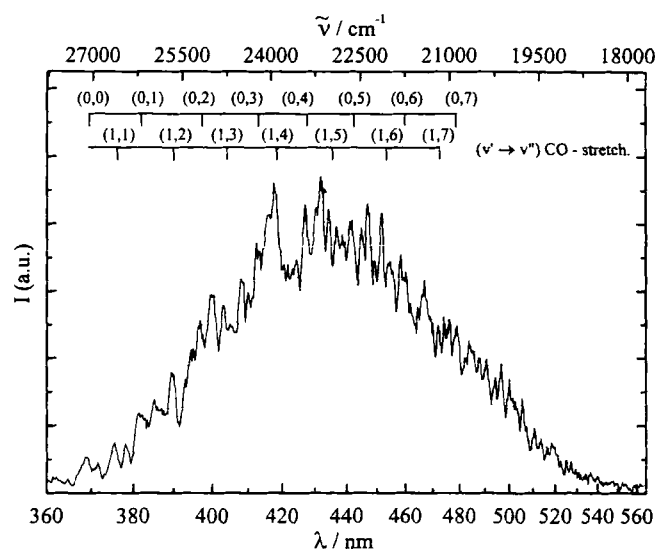


Fig. 3
Fluorescence spectrum of $i\text{-C}_3\text{H}_7\text{O}$ ($\bar{A} \rightarrow \bar{X}$) following excitation in the (4,0)-band at 340.1 nm. Photolysis at 351 nm, $[i\text{-C}_3\text{H}_7\text{ONO}]_0 = 8.0 \times 10^{14} \text{ cm}^{-3}$, $T = 295 \text{ K}$, $p = 80 \text{ mbar}$

As in the case of *i*-propoxy, the identification of the excitation spectrum of *n*-propoxy required the background subtraction of the excitation spectrum of the precursor *n*-propyl nitrite (dotted curve in Fig. 4). Since the overlap of the fluorescence intensity of *n*-propyl nitrite and *n*-C₃H₇O is minimal at the (1,0) transition, *n*-C₃H₇O radicals were excited at 342.4 nm for further LIF studies.

Fig. 5 shows the fluorescence spectrum ($\bar{A} \rightarrow \bar{X}$) of *n*-C₃H₇O after excitation in the (1,0) band. The (0,0) transition can be assigned to the 28684 cm^{-1} band in acceptable agreement with the value obtained from the fluorescence excitation spectrum. The bands show a progression with a separation of $(1000 \pm 50) \text{ cm}^{-1}$ for the CO-stretching vibration in the \bar{X} -state. Hence the bond length seems to be increased in the \bar{A} -state, as in the case of *i*-C₃H₇O. A fluorescence spectrum of *n*-C₃H₇O was previously published by Bai et al. [9]. These authors assigned the (0,0) transition to 29000 cm^{-1} but did not show a fluorescence excitation spectrum for verifying this value. Table 3 lists the spectroscopic constants of propoxy radicals found in this work and values from the literature.

3.2 Lifetime and Quenching Behaviour of Excited Propoxy Radicals

Studies of the quenching behaviour of *n*-C₃H₇O radicals were performed by exciting these radicals in the (1,0)

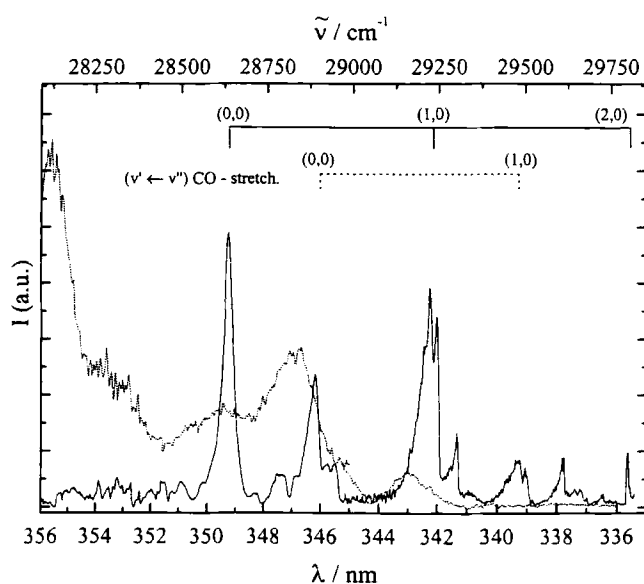


Fig. 4
Fluorescence excitation spectra ($\bar{A} \leftarrow \bar{X}$) of $n\text{-C}_3\text{H}_7\text{O}$ (solid curve) as derived from the observed spectrum following the photolysis of $n\text{-C}_3\text{H}_7\text{ONO}$ at $\lambda=351$ nm after background subtraction of the $n\text{-C}_3\text{H}_7\text{ONO}$ (dotted curve). Intensities have the same scale. $[n\text{-C}_3\text{H}_7\text{ONO}]_0 = 1.0 \times 10^{15} \text{ cm}^{-3}$, $T=295$ K, $[n\text{-C}_3\text{H}_7\text{O}]_0 \approx 2 \times 10^{12} \text{ cm}^{-3}$, $p=13.3$ mbar

Table 2

Band assignment in the fluorescence excitation spectrum ($\bar{A} \leftarrow \bar{X}$) of $n\text{-C}_3\text{H}_7\text{O}$. All transitions are assigned to C-O stretching vibrations. ($v''_{\text{CO}} = 0$; $v''_{\text{unknown vib.}} = 0$)

	$v'_{\text{CO}} =$	0	1	2	3
$\bar{\nu}/\text{cm}^{-1}$	$v'_{\text{unkn.}} = 0$	28 635	29 222	29 796	
$\bar{\nu}/\text{cm}^{-1}$	$v'_{\text{unkn.}} = 1$			28 887	29 474

band at $\lambda=342.4$ nm. N₂, He, O₂ and *n*-propyl nitrite were employed as quenching partners, where O₂ and *n*-propyl nitrite were applied as mixtures diluted in He.

The Stern-Volmer plots obtained for the decay constants of the fluorescence intensities in the presence of each of these collision partners is shown in Fig. 6. Table 4 lists the quenching-rate constants obtained as well as the

Table 3

Summary of spectroscopic properties of propoxy radicals

Radical	T_{00} -transition		$\bar{\nu}_{\text{CO-Stretch.}}/\text{cm}^{-1}$		Ref.
	λ/nm	$\bar{\nu}/\text{cm}^{-1}$	\bar{X}	\bar{A}	
<i>i</i> -C ₃ H ₇ O	368.1	27 167	900±60	560±10	This work
	368.6	27 123		560±10	
	368.5	27 140	960±20		[8]
	368.1	27 168		560	[7]
<i>n</i> -C ₃ H ₇ O	349.2	28 637	1000±50	580±10	This work
	–	29 000 ^{a)}	1065	–	

^{a)} Calculated value

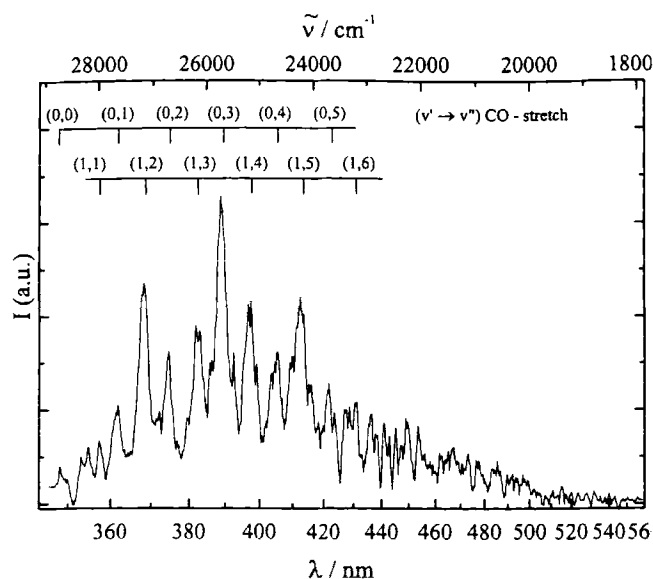


Fig. 5
Fluorescence spectrum of $n\text{-C}_3\text{H}_7\text{O}$ ($\bar{A} \rightarrow \bar{X}$) following excitation in the (1,0)-band at 342.4 nm. Photolysis at 351 nm, $[n\text{-C}_3\text{H}_7\text{ONO}]_0 = 1.5 \times 10^{15} \text{ cm}^{-3}$, $T=295$ K, $p=20$ mbar

collision-free fluorescence lifetimes of the $n\text{-C}_3\text{H}_7\text{O}$ radicals. As has been expected, the collisional quenching of the \bar{A} -state of $n\text{-C}_3\text{H}_7\text{O}$ is particularly fast for *n*-propyl nitrite. However, high rate constants are also observed for O₂, N₂, and He. The results obtained, however, are not inconsistent with quenching efficiencies of these molecules for other alkoxy radicals [9, 10]. From the extrapolations of the individual Stern-Volmer plots a collision free lifetime of $n\text{-C}_3\text{H}_7\text{O}^*$ of $(0.9 \pm 0.05) \mu\text{s}$ is derived. This lifetime is only slightly higher than that obtained by Bai et al. [9] of $(0.7 \pm 0.08) \mu\text{s}$. Both values are close to those derived for CH₃O ($\tau=1.5 \mu\text{s}$ [11]) and C₂H₅O ($\tau=1.0 \mu\text{s}$ [12]), although a systematic trend towards shorter lifetimes with increasing size of the oxy radical is indicated.

Measurements of the radiative lifetimes allow an estimate to be made of the oscillator strength and the absorption coefficient of *n*-propoxy. Using the relation between τ_{rad} and the Einstein coefficients A_{21} and B_{12} we obtain $f=2 \times 10^{-3}$ for the band oscillator strength and $\langle \sigma \rangle = 1.3$

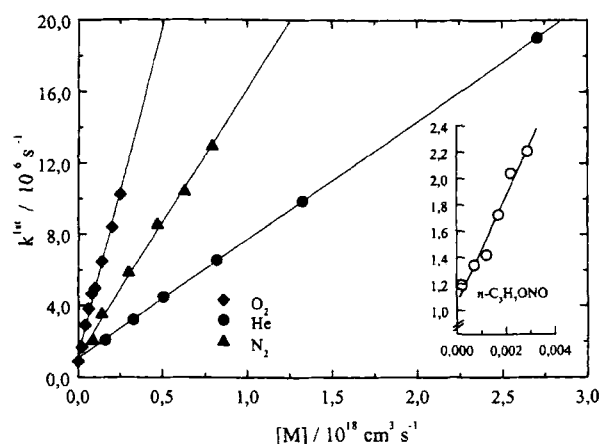


Fig. 6
Stern-Volmer plot for fluorescence quenching of *n*-C₃H₇O* radicals with several collision partners. *T*=295 K, excitation at 342.4 nm

Table 4
Quenching rate constants and collision free fluorescence lifetimes of excited *n*-C₃H₇O

Collision partner	$k_Q/\text{cm}^3 \text{ s}^{-1}$	τ_0/ns
He	$(6.6 \pm 0.2) \times 10^{-12}$	938
N ₂	$(1.5 \pm 0.1) \times 10^{-11}$	845
O ₂	$(4.0 \pm 0.1) \times 10^{-11}$	910
<i>n</i> -C ₃ H ₇ ONO	$(4.1 \pm 0.3) \times 10^{-10}$	950

$\times 10^{-17} \text{ cm}^2$ for the average absorption coefficient of the ($\bar{A} \leftarrow \bar{X}$) band between 341.8–342.7 nm.

As opposed to *n*-C₃H₇O* the quenching experiments performed on *i*-C₃H₇O* after excitation in the (4,0) band generally lead to different results. Whereas with O₂ as a collision partner a normal quenching behaviour with $k_a = (1.9 \pm 0.2) \times 10^{-11} \text{ cm}^3 \text{ s}^{-1}$, comparable to the corresponding quenching rate coefficient of O₂ for *n*-C₃H₇O*, was observed, all other quench gases (N₂, He and *i*-propyl nitrite) produced an extension of the fluorescence lifetime with increasing collider pressure. Fig. 7 shows the results obtained for M=He. As can be seen the first order fluorescence decay constant decreases rapidly with increasing He pressure in the range $(1-10) \times 10^{17} \text{ cm}^{-3}$, but becomes essentially independent on [M] above this pressure. Similar observations were made for M=N₂ and *i*-propyl nitrite.

The inverse pressure effect on the *i*-propoxy fluorescence lifetime may be explained by higher vibronic excitation of the \bar{A} -state followed by competitive vibronic deexcitation and predissociation, viz.

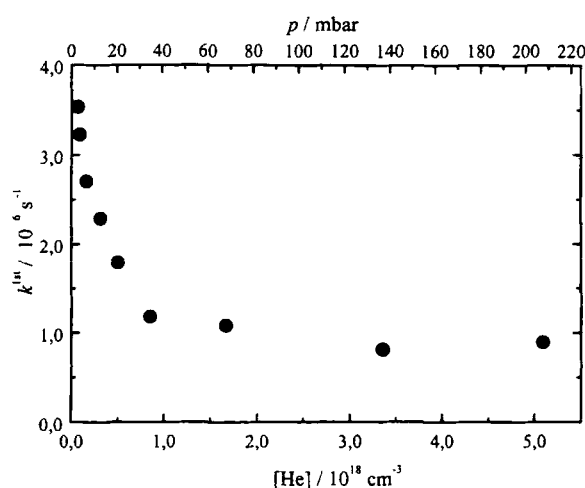
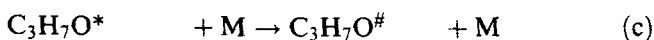
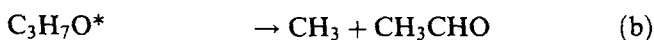
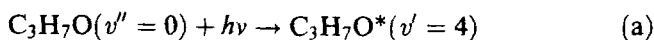
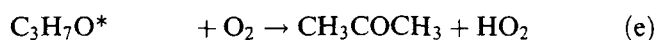


Fig. 7
Variation of the observed radiative decay constant of *i*-C₃H₇O* versus He concentration. *T*=295 K, excitation at $\lambda_{\text{exc.}} = 340.1 \text{ nm}$

As a result of this mechanism increasing collider pressure may lead to increased fluorescence lifetime, as observed for M=He, N₂ and *i*-propyl nitrite. Since this effect is noticeable in the pressure regime $(1-10) \times 10^{17} \text{ cm}^{-3}$, the rate coefficients k_b , $k_c[\text{M}]$ and k_d must be of the same order of magnitude in this pressure range. Assuming $k_d \approx 2 \times 10^6 \text{ s}^{-1}$, this predicts $k_c \approx (0.2-2) \times 10^{-11} \text{ cm}^3 \text{ s}^{-1}$ for the second order rate coefficient for vibrational deactivation of the *i*-propoxy \bar{A} -state.

As opposed to M=He, N₂ and *i*-propyl nitrite an inverse pressure effect on the *i*-propoxy fluorescence lifetime was not observed for M=O₂. This behaviour may be explained by reactive deexcitation of *i*-propoxy, viz.



This process prevents collisional population of longer lived fluorescing states of *i*-C₃H₇O[#] with lower vibrational excitation.

3.3 The Reaction of *i*- and *n*-Propoxy Radicals with (1) O₂

First-order rate constants for reaction of *i*- and *n*-propoxy radicals with O₂ were obtained from plots of LIF signal intensities versus time delay between the photolysis and excitation-laser beam. The O₂-concentration range was limited to $0.5-3.0 \times 10^{17} \text{ cm}^{-3}$ due to fluorescence quenching at high concentrations and to undetectable reaction rates at lower concentrations, respectively. Fig. 8 shows a typical second order plot for the reaction of *i*-propoxy with O₂ at two different temperatures. The slope provides the rate-constant for the reaction to be investigated and the intercept shows the sum of all removal processes other than reaction with O₂, namely diffusion out of the observation volume and, mainly, reaction with NO. According to the empirical rules [13] of the relative im-

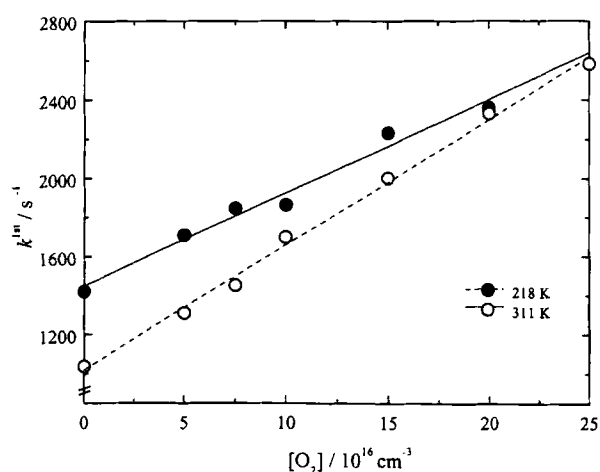


Fig. 8
Dependence of the first order decay constants of the reaction $i\text{-C}_3\text{H}_7\text{O} + \text{O}_2 \rightarrow \text{products}$ on the O_2 -concentration for two temperatures. $p = 13$ mbar, excitation at 340.1 nm

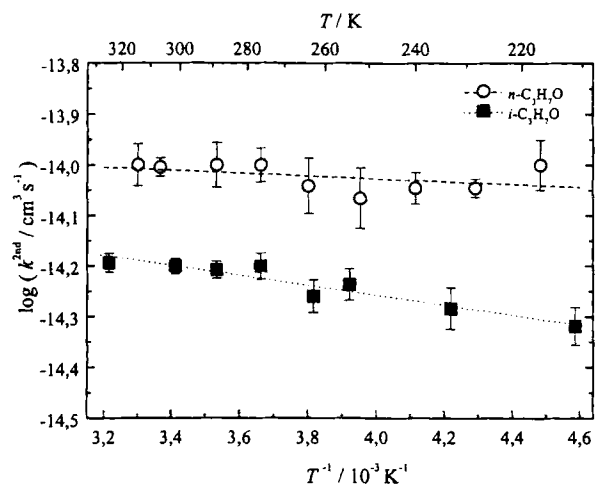


Fig. 9
Arrhenius representation of the rate coefficient for $i\text{-C}_3\text{H}_7\text{O} + \text{O}_2 \rightarrow \text{products}$ ($p = 13$ mbar) and for $n\text{-C}_3\text{H}_7\text{O} + \text{O}_2 \rightarrow \text{products}$ ($p = 20$ mbar)

portance of the reaction with O₂ versus decomposition, decomposition of the propoxy radicals plays a minor role.

Rate constants for the reactions of *i*- and *n*-propoxy with O₂ were measured in the temperature range 218–313 K (*i*-C₃H₇O) and 223–303 K (*n*-C₃H₇O). Fig. 9 shows the corresponding Arrhenius plots, from which the expressions:

$$k_1(i) = (1.0 \pm 0.3) \times 10^{-14} \exp(-1.8 \pm 0.4 \text{ kJ mol}^{-1}/RT) \text{ cm}^3 \text{ s}^{-1}$$

$$k_1(n) = (1.4 \pm 0.6) \times 10^{-14} \exp(-0.9 \pm 0.5 \text{ kJ mol}^{-1}/RT) \text{ cm}^3 \text{ s}^{-1}$$

were derived.

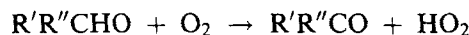
The rate coefficient for the reaction of *i*-propoxy radicals with O₂ has previously been determined by Balla et

Table 5
Arrhenius parameters for the reaction of several alkoxy radicals with O₂

	$\log(A/\text{cm}^3 \text{ s}^{-1})$	$E_a/\text{kJ mol}^{-1}$	Ref.
CH ₃ O	-13.14	9.0	[2]
C ₂ H ₅ O	-13.1	4.6	[15]
<i>i</i> -C ₃ H ₇ O	-13.9	1.8±0.4	This work
<i>i</i> -C ₃ H ₇ O	-13.8	1.6	[4]
<i>n</i> -C ₃ H ₇ O	-13.9	0.9±0.5	This work

al. [4] using a technique similar to the one used in the present study. Although there is a 10% discrepancy in the activation energy reported, the absolute values of the rate coefficients agree within the error limits. As opposed to *i*-propoxy radicals, no literature data of direct measurements are available for comparison with the present work for the reaction of *n*-propoxy radicals with O₂. The values available were obtained by relative measurements [3, 5].

Alkoxy radicals are generally assumed to react with O₂ in pressure independent bimolecular H-abstraction reactions, viz.



However, as noted previously [15] and confirmed by the present study, *A*-factors for these reactions are unusually low and not consistent with a loose R'R''C(O)··H··O₂ transition state. Table 5 summarizes Arrhenius-parameters for reactions of C₁–C₃ alkoxy radicals with O₂. As can be seen, none of the *A*-factors exceeds 10⁻¹³ cm³ s⁻¹. Several attempts have been made to rationalize these findings. Hartmann and Zellner [15] have discussed the possibility of a complex bimolecular reaction including the intermediate formation of a R'R''CH(O)O₂ adduct. However, due to the apparent endothermicity of this step, this possibility was rejected. Instead, these authors suggested that a tight and late transition state with the C··H··O₂ moiety in bent configuration could explain the low *A*-factors. It should be noted that a somewhat lower preexponential factor for the reaction between *n*-propoxy and O₂, $A = (2.1\text{--}4.2) \times 10^{-13} \text{ cm}^3 \text{ s}^{-1}$, was predicted by Zabarnick and Heicklen [14]. This value, however, is not confirmed by the present study.

3.4 The Reaction of *i*- and *n*-Propoxy Radicals with (2) NO₂

All kinetic investigations on reaction (2) were performed at 296 K. Second order rate constants were obtained as described above. The NO₂ concentration was varied in the range (0.2–1.8) × 10⁻¹⁴ cm⁻³. The total pressure was varied within the range 6.7–53 mbar (*n*-C₃H₇O) and 6.7–106 mbar (*i*-C₃H₇O). The resulting rate coefficients are summarized in Fig. 10. As can be seen, the data do not exhibit a significant pressure effect. As a result, the following rate coefficients at 296 K are derived:

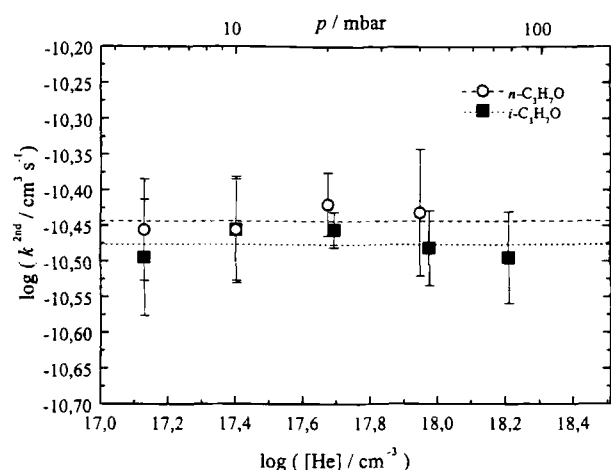


Fig. 10
Dependence of second order rate constants for $i\text{-C}_3\text{H}_7\text{O} + \text{NO}_2 \rightarrow \text{products}$ and $n\text{-C}_3\text{H}_7\text{O} + \text{NO}_2 \rightarrow \text{products}$ on total pressure. $T = 295 \text{ K}$, $[i\text{-C}_3\text{H}_7\text{ONO}]_0 = 1.5 \times 10^{14} \text{ cm}^{-3}$, $[n\text{-C}_3\text{H}_7\text{ONO}]_0 = 1.3 \times 10^{15} \text{ cm}^{-3}$

$$k_2(i) = (3.3 \pm 0.3) \times 10^{-11} \text{ cm}^3 \text{ s}^{-1}$$

$$k_2(n) = (3.6 \pm 0.4) \times 10^{-11} \text{ cm}^3 \text{ s}^{-1}$$

The value for *i*-propoxy is consistent with the value of $k_i = (3.68 \pm 0.16) \times 10^{-11} \text{ cm}^3 \text{ s}^{-1}$ as obtained by Balla et al. [4]. These authors observed a dependence of the rate constant on the photolysis energy which they explained with the reaction of *i*-propoxy with O(³P), formed in the photolysis of NO₂. A similar observation, however, has not been made in the present study, because lower (<20 mJ) laser pulse energies were used.

The reaction of alkoxy radicals with NO₂ may proceed via two channels, namely (h) addition of NO₂ and (i) abstraction of a hydrogen atom [3]:



In the present work no distinction between the two channels can be made and only the sum of the rate constants, $k_2 = k_h + k_i$, is measured. Moreover, the absence of a pressure effect also does not provide a hint as to which channel is dominant. However, Atkinson et al. [16] estimate $k_i/k_h < 0.2$, which together with the present observation indicates, that the addition reaction (h) has reached its high pressure limit at all pressures applied (i.e. $p > 6 \text{ mbar}$).

4. Summary and Conclusion

LIF studies of *i*-propoxy radicals and *n*-propoxy radicals were performed and fluorescence excitation spectra and fluorescence spectra of both radicals were obtained. Reaction rate constants of these radicals with O₂ and NO₂ were measured. The temperature dependences of their

reactions with O₂ showed small positive activation energies but low preexponential factors. Rate constants for the reactions with NO₂ at $T = 296 \text{ K}$ did not show a significant pressure effect. Despite the relatively low rate coefficient for reaction of *i/n*-propoxy with O₂, this reaction is the most important pathway of propoxy radicals under tropospheric conditions due to the high O₂-concentration. The reaction with NO₂ becomes only significant in heavily polluted areas with high NO₂-concentrations.

Support of this work by "Fonds der Chemischen Industrie" and by BMBF is gratefully acknowledged.

References

- [1] D. Gutman, N. Sanders, and J.E. Butler, Kinetics of the Reactions of Methoxy and Ethoxy Radicals with Oxygen, *J. Phys. Chem.* **86**, 66–70 (1982).
- [2] K. Lorenz, D. Rhäsa, and R. Zellner, Laser photolysis – LIF kinetic studies of CH₃O and CH₂CHO with O₂ between 300 and 500 K, *Ber. Bunsenges. Phys. Chem.* **89**, 341 (1985).
- [3] J. Heicklen, The Decomposition of Alkyl Nitrites and the Reactions of Alkoxy Radicals. *Adv. Photochem.* **14**, 177–272 (1988).
- [4] R.J. Balla, H.H. Nelson, and J.R. McDonald, Kinetics of the Reactions of Isopropoxy Radicals with NO, NO₂ and O₂, *J. Chem. Phys.* **99**, 323–335 (1985).
- [5] S. Zabarnick and J. Heicklen, Alkoxy Radicals II: *n*-C₃H₇O Radicals, *Int. J. Chem. Kin.* **17**, 477–501 (1985).
- [6] G.D. Mendenhall, D.M. Golden, and S.W. Benson, The Very-Low-Pressure Pyrolysis (VLPP) of *n*-Propyl Nitrate, *tert*-Butyl Nitrite, and Methyl Nitrite. Rate Constants for Some Alkoxy Radical Reactions. *Int. J. Chem. Kin.* **7**, 725 (1975).
- [7] S.C. Foster, Y.C. Hsu, C.P. Damo, X. Liu, C.Y. Kung, and T.A. Miller, Implications of the Rotationally Resolved Spectra of the Alkoxy Radicals for their Electronic Structure, *J. Phys. Chem.* **90**, 6766–6769 (1986).
- [8] J. Bai, H. Okabe, and B. Halpern, Fluorescence Spectrum and Lifetime of the *i*-C₃H₇O Radical, *Chem. Phys. Lett.* **149**, 37–39 (1988).
- [9] J. Bai, H. Okabe, and M.K. Emadi-Babaki, Fluorescence Spectrum and Lifetime of *n*-C₃H₇O Radicals, *J. Photochem. Photobiol. A: Chemistry* **50**, 163–169 (1989).
- [10] K. Ohbayashi, H. Akimoto, and I. Tanaka, Emission Spectra of CH₃O, C₂H₅O and *i*-C₃H₇O Radicals, *J. Phys. Chem.* **81**, 798–802 (1977).
- [11] G. Inoue, H. Akimoto, and M. Okuda, Laser-Induced Fluorescence Spectra of CH₃O, *Chem. Phys. Lett.* **63**, 213 (1979).
- [12] G. Inoue, H. Akimoto, and M. Okuda, Laser-induced Fluorescence of the C₂H₅O Radical, *J. Chem. Phys.* **75**, 2060 (1980).
- [13] R. Atkinson and W.P.L. Carter, Reactions of Alkoxy Radicals Under Atmospheric Conditions: The Relative Importance of Decomposition Versus Reaction with O₂, *J. Atm. Chem.* **13**, 195–210 (1991).
- [14] S. Zabarnick and J. Heicklen, Reactions of Alkoxy Radicals with O₂. I. C₂H₅O Radicals, *Int. J. Chem. Kin.* **17**, 455 (1985).
- [15] D. Hartmann and R. Zellner, Kinetics and HO₂ Product Yield of the Reaction C₂H₅O+O₂ between 295 and 411 K, *Ber. Bunsenges. Phys. Chem.* **94**, 639–645 (1990).
- [16] R. Atkinson, Evaluated and Photochemical Data for Atmospheric Chemistry Supplement IV, *J. Phys. Chem. Ref. Data* **21**, 1125 ff. (1992).

(Received: December 3, 1997
final version: February 27, 1998)

E 9761